

PROCESSES IN CONDENSED INERT GASES INVOLVING EXCESS ELECTRONS

E. B. Gordon^a, *B. M. Smirnov*^{b*}

^a*Institute of Problems of Chemical Physics Russian Academy of Sciences
142432, Chernogolovka, Moscow Region, Russia*

^b*Institute for High Temperatures Russian Academy of Sciences
127412, Moscow, Russia*

Submitted 17 December 2003

Drift of an excess electron in dense and condensed inert gases in external electric field and excitation of atoms by electron impact in these systems are analyzed. The effective potential energy surface for an excess electron at a given electric field strength consists of wells and hills, and the actions of neighboring atoms are therefore separated by saddles of the potential energy. At the atomic densities such that the difference of interaction potentials for an excess electron between neighboring wells and hills of the potential energy surface becomes small, the electron mobility is large. This is realized for heavy inert gases (Ar, Kr, Xe) with a negative scattering length of the electron on individual atoms. In these cases, the average potential energy of the electron interaction with atoms corresponds to attraction at low atomic densities and to repulsion at high densities. The transition from attraction to repulsion at moderate atomic densities leads to the maximum of the electron mobility. A gas model for the electron drift in condensed inert gases is constructed on the basis of this character of interaction. Due to high electron mobility, condensed inert gases provide high efficiency of transformation of the electric field energy into the energy of emitting photons through drifting electrons. It is shown that although the role of formation of autodetaching states in the course of the electron drift is more important for condensed inert gases than for rare gases, this effect acts weakly on exciton production at optimal atomic densities. The parameters of a self-maintained electric discharge in condensed inert gases as a source of ultraviolet radiation are discussed from the standpoint of electron drift processes.

PACS: 34.80.-i, 52.80.Wq, 52.80.Yr, 79.20.Kz

1. INTRODUCTION

The mobility K and drift velocity w of a free electron in gases is inversely proportional to the number density N of atoms, i.e., the quantities KN and wN in a gas are independent of its density. At high densities, this law is violated because of two reasons. First, electron scattering proceeds simultaneously on several atoms, and second, the interaction between atoms changes the atomic system, which affects the character of the electron interaction in this system. For inert gases, where atoms conserve their individuality in a condensed system, the behavior of an excess electron injected in a condensed gas is different depending on its sort. In light inert gases, He and Ne, an excess electron compels to displace the surrounding atoms. This structure change moves together with the electron, and

therefore the electron effective mass is of the order of the atomic mass, and hence the reduced electron mobility KN in these condensed gases (He and Ne) is essentially lower than in gases.

As follows from experiments [1–15], different behavior of the reduced electron mobility occurs in heavy inert gases, Ar, Kr, and Xe. The electron effective mass in condensed heavy inert gases is of the order of the free electron mass, and as the atomic number density increases, the reduced mobility has a tendency to decrease; it experiences a sharp jump in a narrow range of the atomic number densities (see Fig. 1 for the case of xenon [7, 11]). Table 1 [16] demonstrates this behavior of the mobility of the excess electron. In Table 1, K_{gas} is the electron zero-field mobility in gases at room temperature, K_{tr} is the electron zero-field mobility at the triple point, and K_{max} is the maximum electron zero-field mobility for the liquid state. This table also

*E-mail: smirnov@orc.ru, smirnov@oivtran.iitp.ru

Table 1. Parameters of drift of an excess electron in rare gases

	Ar	Kr	Xe
T_{max}, K	155	170	223
$N_{max}, 10^{22} \text{ cm}^{-3}$	1.2	1.4	1.2
$K_{max}N_{max}, 10^{24}(\text{cm} \cdot \text{V} \cdot \text{s})^{-1}$ [14]	22	64	72
T_{tr}, K	85	117	163
$N_{liq}, 10^{22} \text{ cm}^{-3}$	2.1	1.8	1.4
$K_{tr}N_{liq}, 10^{24}(\text{cm} \cdot \text{V} \cdot \text{s})^{-1}$ [1-6, 8, 10, 14]	10 ± 1	29 ± 5	28 ± 10
V_0, V [9, 12, 13, 15]	-0.3	-0.5	-0.8
$K_{gas}N, 10^{23}(\text{cm} \cdot \text{V} \cdot \text{s})^{-1}$ [16]	12	0.62	0.17

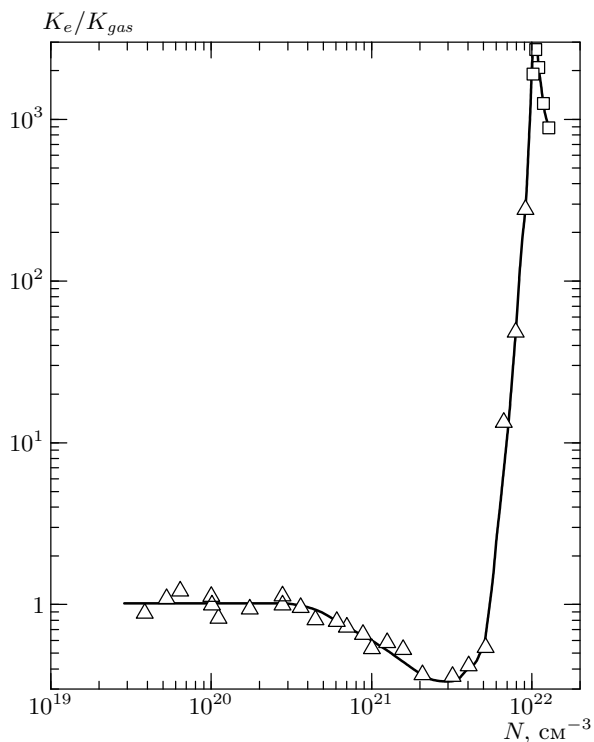


Fig. 1. The dependence of the reduced electron mobility in xenon on the density of atoms according to experiments [7, 11]

contains the temperatures T_{max} of the maximum electron mobility and the triple point temperatures T_{tr} and the number densities of atoms N_{max}, N_{liq} corresponding to these temperatures. We note that the difference of the electron mobilities for the solid and liquid inert gases is not significant, i.e., high mobility of an excess

electron cannot be explained by the order distribution of atoms. The quantity V_0 in Table 1 is the difference of the electric potentials acting on the electron if it is located inside and outside a condensed inert gas. It is energetically profitable for an excess electron to be located inside the inert gas, and the minimum of V_0 corresponds to the atomic number densities that are related to the maximum of the electron mobility. In addition, high mobility of an excess electron is observed only in a narrow range of atomic number densities, to be considered below. As follows from the data in Table 1, the maximum reduced mobilities of the excess electrons in inert gases, as well as the reduced mobilities at the triple point, significantly exceed those at gaseous densities. This difference is especially high for xenon, which is the main object of our consideration. In addition, the maximum reduced electron mobilities in inert gases exceed those in metals of high conductivity. Indeed, the reduced electron mobility $K_e N_a$ is equal to 2.9 and 3.1 in the units $10^{24} (\text{cm} \cdot \text{V} \cdot \text{s})^{-1}$ for copper and silver respectively. We note that because electrons are degenerate in these metals, a typical electron velocity near the Fermi surface is much greater than the thermal velocity of a free electron. Therefore, although the specific mobilities of an excess electron in condensed inert gases significantly exceed those in metals, the ratios of the electron free mean path to the distance between nearest atoms (or the lattice constant) have the same order of magnitude for both condensed inert gases and metals.

Some theories [17-21] explain high mobility of an excess electron by the Ramsauer effect in electron scattering on an individual atom, but such approaches are just models because they are correct only for gases. Of

course, the gaseous approach for the electron scattering is the simplest one, but it does not allow us to describe the electron behavior in a wide range of atomic number densities with a small number of fitting parameters. The high mobility of an excess electron in condensed inert gases has a fundamental meaning because it is an evidence of a weak interaction between the electron and this matter at such densities. In what follows, we consider just this range of the atom number densities corresponding to high values of the electron mobility, and our task is to explain the nature of this phenomenon. Analyzing the properties of the total potential energy that acts on the electron from a condensed inert gas, we show that it varies in average from attraction to repulsion, as the atomic number density increases. The maximum electron mobility corresponds to the transition from attraction to repulsion, and we analyze the problem of drift of an excess electron in condensed inert gases from this standpoint in what follows.

The high mobility of excess electrons corresponds to a low resistance of condensed inert gases at such atom number densities if the excess electrons propagate in this matter under the action of an external electric field. When the electron energy reaches the threshold of atom excitation, it is consumed to formation of excitons; in this range of atom number densities, formation of excitons by electron impact is an effective process. But formation of autodetachment states may affect the efficiency and rate of exciton formation in condensed inert gases. These autodetachment states are bound states of excited and excess electrons with the binding energy about 0.4 eV [22]. Formation of autodetachment states of inert gas atoms impedes excitation of atoms, and we consider this problem below.

The high electron mobility in condensed inert gases has the fundamental meaning and can be applied for transformation of the energy of an external electric field into the energy of photons in the vacuum ultraviolet (VUV) spectrum range through excess electrons moving in condensed inert gases. This method, which requires the creation of a self-maintaining electric discharge in condensed inert gases, was suggested in [23, 24] and was then experimentally proved for xenon [25–27]. Because the excited inert gas atoms are characterized by a high excitation energy, such a method allows effectively converting the electric energy into radiation because elastic scattering of electrons is weak. This problem of energy conversion is analyzed in this paper in the context of the behavior of excess electrons inside condensed inert gases.

2. INTERACTION OF AN EXCESS ELECTRON IN CONDENSED INERT GASES

The peculiarity of condensed inert gases is a small binding energy between atoms in comparison with typical atomic energies. This implies that the interaction between neighboring atoms in the solid and liquid inert gases is relatively small and allows us to use the similarity law for various parameters of dense and condensed inert gases [28]. The reason for this is that the parameters of inert gases are governed by pairwise interactions of atoms, and the pair interaction potentials are known for inert gas atoms with a high (several percent) accuracy [29–32]. The pair character of the atom interaction allows expressing some parameters of inert gases through the parameters of the interaction potential of two atoms and provides the validity of the scaling laws for various parameters of bulk inert gases. Representing the pair interaction potential of two atoms in the form of a potential well, we use two interaction parameters, the depth D of this potential well, and the equilibrium interatomic distance R_e that corresponds to the minimum of the interaction potential. Table 2 gives some reduced parameters of heavy inert gases [28] and confirms the validity of the similarity law for them. Here, a is the lattice constant, and all the inert gases have the face-centered cubic lattice, T_{tr} is the triple-point temperature, V_{liq} and V_{sol} are the specific volumes per atom for the liquid and solid states respectively at the triple point, ε_{sub} is the sublimation energy per atom for the crystal at the triple point, ΔH_{fus} is the fusion energy (the energy consumed to melting) per atom, ΔS_{fus} is the entropy jump per atom at melting, and r_W is the Wigner–Seitz radius for the liquid state. As follows from Table 2, the reduced parameters are the same for different rare gases within the accuracy of several percent. Hence, the bound systems of inert gas atoms have a simple nature and can be treated as systems of classical bound atoms. We use this in the subsequent analysis.

Although scaling is not valid for an electron in condensed inert gases, it is convenient to express the reduced parameters of an excess electron, which allows us to compare the electron parameters with those for the interaction of atoms. The number densities N_{sol} and N_{liq} (where $N_{sol} = 1/V_{sol}$ and $N_{liq} = 1/V_{liq}$) in Table 3 correspond to the solid and liquid states of inert gases at the triple point, N_{max} is the number density in Table 1 at which the zero-field electron mobility has the maximum, $N_0 = R_e^{-3}$, and $N_* = \sqrt{2}/(2\bar{r})^3$, where \bar{r} is the mean radius of the valence electron in a given

Table 2. Parameters of the interaction potential of two identical atoms of inert gases (R_e, D) and reduced parameters of condensed inert gases near the triple point [28]

	Ar	Kr	Xe	Average
$R_e, \text{Å}$	3.76	4.01	4.36	–
D, K	143	200	278	–
$a, \text{Å}$	3.755	3.992	4.335	–
a/R_e	1.00	0.99	1.01	1.005 ± 0.013
$N_0 = R_e^{-3}, 10^{22} \text{ cm}^{-3}$	1.88	1.55	1.21	–
T_{tr}/D	0.587	0.578	0.570	0.579 ± 0.007
$\rho_{tr} R_e^3/D, 10^{-3}$	1.9	1.7	1.7	1.9 ± 0.2
V_{liq}/R_e^3	0.879	0.884	0.855	0.88 ± 0.02
V_{sol}/R_e^3	0.77	0.76	0.74	0.76 ± 0.01
ε_{sub}/D	6.5	6.7	6.7	6.5 ± 0.3
$\Delta H_{fus}/D$	0.990	0.980	0.977	0.98 ± 0.02
ΔS_{fus}	1.69	1.70	1.71	1.68 ± 0.03
r_W/R_e	0.639	0.641	0.627	0.64 ± 0.01

Table 3. Reduced parameters of an excess electron inside condensed inert gases

	Ar	Kr	Xe
N_{sol}/N_0	1.30	1.31	1.34
N_{liq}/N_0	1.13	1.13	1.17
N_{max}/N_0	0.68	0.90	0.99
N_*/N_0	2.05	1.54	1.38
eV_0/ε_{sub}	–3.8	–4.3	–4.9

atom and the values of these radii are taken from [33–35]. Hence, N_* is the number density of balls of radius \bar{r} if these balls form the crystal lattice of close packing. In accordance with the Pauli exchange interaction, an excess electron cannot be located inside atoms, and as follows from the data in Table 3, the excluded volume for location of an excess electron is comparable to the total volume inside condensed inert gases at the triple point. As can be seen, the similarity law is not valid for N_*/N_0 . In addition, the ratio N_{liq}/N_* grows as we transfer from Ar to Xe; this ratio expresses a typical part of space inside a liquid inert gas where an excess electron may not be located.

We now consider the problem of interaction of an excess electron inside a liquid inert gas from another

standpoint, analyzing the behavior of the potential energy surface for this electron as the atom density increases starting from low values. At low atomic densities, when an electron is located in a gas, it interacts with individual atoms independently. In regions between atoms far from them, the interaction potential is zero, and nonzero interaction occurs only near regions occupied by atoms. On the basis of the Fermi formula [36], the interaction potential between the electron and atoms can be presented as

$$U(\mathbf{r}) = \sum_i \frac{2\pi\hbar^2}{m_e} L\delta(\mathbf{r} - \mathbf{R}_i), \quad (1)$$

where \mathbf{r} is the electron coordinate, \mathbf{R}_i is the coordinate of the i th atom, and L is the electron–atom scattering length. Because the scattering length is negative for Ar, Kr, and Xe, this interaction potential corresponds to attraction in regions where atoms are located. Therefore, the potential energy surface consists of regions inside atoms with a sharp electron repulsion, regions near each atom with electron attraction, and regions between atoms with zero interaction potential. The region between atoms with zero interaction potential shrinks as the number density of atoms increases, and when the distance between the nearest neighbors is comparable with the electron orbit size, the potential energy surface takes the form of wells and saddles, which separate regions of individual atoms. This potential energy surface resembles that describing inter-

action of bound atoms in clusters [37, 38]. In reality, attraction corresponds only to an average interaction of an electron of zero energy with an individual atom in a gas, and it leads to a red shift of spectral lines emitted by excited atoms located in inert gases [39]. The exchange interaction of a test electron with electrons of the inert gas atoms is accompanied by repulsion if this electron penetrates an internal atom region occupied by other electrons. The volume of repulsion near each atom is approximately $1/N_*$, where the values of N_* are given in Table 3, and this implies that high electron mobility is absent at high gas pressures.

The interaction potential between a test electron and an individual inert gas atom can therefore be composed of repulsion at small distances from the atom and attraction at longer distances, which are of the order of the electron scattering length. Correspondingly, the attraction in the region of location of individual atoms dominates in the interaction potential of a test electron with the system of inert gas atoms at low densities of atoms. Evidently, as the number density of atoms increases, the attraction part of the interaction potential disappears, and therefore there is an atomic density when the average interaction potential becomes zero. This atomic density corresponds to the transition from attraction to repulsion for the total interaction potential, and the mobility of slow electrons obtains a maximum, because a typical energy difference between wells or hills in the potential energy becomes minimal at such an atomic density. This electron behavior is expected, however, if the electron scattering length on an individual atom is negative, i.e., for Ar, Kr, Xe.

Thus, there is a strong repulsion of an excess electron in heavy inert gases near each core due to the exchange interaction with internal atomic electrons, and a test electron does not penetrate the atom because of the Pauli exclusion principle. An average electron interaction with an individual atom corresponds to attraction because of a negative electron–atom scattering length. At intermediate atomic densities, these interactions compensate each other in average, and the electron mobility has a maximum at such densities. We are guided by the liquid state of condensed inert gases, because the order distribution of atoms is not of principle for the nature of this high electron mobility. Therefore, the electron mobilities for the solid and liquid states do not differ in principle, but this mechanism of high electron mobility corresponds to a narrow density range, while high mobility of a solid inert gas can be observed in a wide range of atomic densities.

3. DRIFT AND MOBILITY OF AN EXCESS ELECTRON IN HEAVY INERT GASES

Guided by a range of high mobilities of an excess electron in condensed inert gases where the interaction of this electron with the environment is weak, we use a gas approach for electron scattering. Keeping in mind that the potential energy surface for an individual electron consists of wells and hills, and hills separate the action of an individual core, we use the gaseous approach for the electron scattering such that each core is a scattering center for an excess electron. If the cross section for scattering on an individual core is small compared to the square atom size, we reduce the problem of electron motion inside a condensed inert gas to scattering on individual cores, as it takes place in gases. We note that this model is valid only in the case of a high electron mobility in a condensed system, if the electron interaction with this system is weak.

In the case of electron motion in a gas, when a test electron is scattered subsequently on individual atoms, the zero-field electron mobility K_e is given by [40, 41]

$$K_e = \frac{e}{3m_e} \left\langle \frac{1}{v^2} \frac{d}{dv} \left(\frac{v^3}{\nu} \right) \right\rangle, \quad (2)$$

where m_e is the electron mass, v is the electron velocity, averaging is taken over the distribution of electrons with respect to velocities, $\nu = Nv\sigma^*$ is the rate of the electron–atom scattering, with N being the atom number density, and σ^* is the diffusion cross section of the electron–atom elastic scattering. For simplicity, we below consider the case where the cross section is independent of the collision velocity and formula (2) takes the form [40, 41]

$$K_e = 0.53 \frac{e\lambda}{\sqrt{m_e T}}, \quad \text{or} \quad K_e N = 0.53 \frac{e}{\sigma^* \sqrt{m_e T}}, \quad (3)$$

where $\lambda = (N\sigma^*)^{-1}$ is the mean free path of the electron in a gas and T is the temperature. This connection of the reduced electron mobility and the scattering cross section allows us to express the diffusion cross section σ^* of the electron–atom scattering in a gas through the reduced mobility, which is given by

$$\sigma^* = \frac{0.5}{\sqrt{m_e T} K_e N}. \quad (4)$$

In particular, applying this gas model to gaseous xenon and using the experimental values [7] of the reduced mobility $K_e N = 3 \cdot 10^{22} (\text{cm} \cdot \text{V} \cdot \text{s})^{-1}$ at the temperature $T = 236 \text{ K}$, we obtain from formula (4) the diffusion cross section $\sigma^* = 52 \text{ \AA}^2$ at this temperature. We introduce the critical number density of atoms N_{cr}

Table 4. Parameters of the gas model for drift of an excess electron in liquid rare gases [16]

	Ar	Kr	Xe
$\sigma_{tr}/\pi a_{tr}^2$	0.012	0.005	0.005
$\sigma_{max}/\pi a_{max}^2$	0.004	0.002	0.002
λ_{tr}/a_{tr}	65	150	170
λ_{max}/a_{max}	200	450	480

that characterizes the transition from the gaseous system to the condensed one and corresponds to the relation $\sigma^* = \pi r_W^2$, where r_W is the Wigner–Seitz radius ($\pi r_W^2 = 2.3 \cdot 10^{-15}$ cm² for liquid xenon). According to formula (4), the critical number density is

$$N_{cr} = \frac{3\sqrt{\pi}}{4(\sigma^*)^{3/2}}, \quad (5)$$

and it is equal to $N_{cr} = 4 \cdot 10^{21}$ cm⁻³ for xenon. This is the transient gas–liquid number density for xenon.

We treat the density range of the maximum electron mobility in xenon on the basis of the gas model. Taking the maximum zero-field electron mobility from Table 1 ($K_e N = 7.2 \cdot 10^{25}$ (cm·V·s)⁻¹ at the atom number density $N_{max} = 1.2 \cdot 10^{22}$ cm⁻³), we obtain on the basis of formula (4) that $\sigma^* = 1.4 \cdot 10^{-18}$ cm², which is small in comparison with $\pi r_W^2 = 2.3 \cdot 10^{-15}$ cm², and hence the gas model is applicable in this case. Thus composing electron scattering in a condensed inert gas at the atomic density of the maximum electron mobility as a result of the electron interaction with small independent scatterers located on atom cores, we use formula (4) to find the diffusion cross sections for electron scattering σ_{max} and σ_{tr} that correspond to the atom number densities N_{max} and N_{tr} (see Table 1). These cross sections are given in Table 4 [16], where a_{tr} and a_{max} are the distances between nearest neighbors at these atomic densities, and λ_{max} and λ_{tr} are the electron mean free paths for these densities. As can be seen, the gas approach is valid because the effective cross sections are relatively small, whereas the mean free paths for electrons are relatively large.

We consider the data in Table 1 from another standpoint, composing the potential energy surface for an excess electron in the form of wells and hills near each core, if the well depth is relatively small. We take the interaction potential of the electron with each atomic center in the form

$$U(r) = -U_0 \exp\left(-\frac{r^2}{a^2}\right), \quad a \leq r_W, \quad (6)$$

where r is the distance from the atom center, a is the range of atomic forces, and r_W is the Wigner–Seitz radius for the condensed system. The electron scattering on an individual center is weak if $U_0 \ll \varepsilon$, where ε is the electron energy. We can then use the perturbation theory for electron scattering. This amounts to the Born approximation, and the differential cross section of the electron scattering on an individual center in the Born approximation for the interaction electron–core potential (6) is [42]

$$d\sigma = \frac{\pi a^2}{4} \left(\frac{m_e U_0 a^2}{\hbar^2}\right)^2 \exp\left(-\frac{K^2 a^2}{2}\right) d\Omega, \quad (7)$$

where

$$K = 2q \sin(\theta/2)$$

is the variation of the electron wave vector as a result of scattering, θ is the scattering angle, q is the initial electron wave vector, and

$$d\Omega = \pi d \cos \theta$$

is the solid angle element. From this, we have the diffusion cross section of elastic scattering on each scattered center given by

$$\sigma^* = \frac{\pi^2 a^2}{16} \left(\frac{U_0}{\varepsilon}\right)^2. \quad (8)$$

This consideration is valid for $U_0 \ll \varepsilon$, i.e., in the range of parameters where the electron mobility is high in a condensed system. In the case of xenon at the atomic density of the maximum electron mobility, we obtain $U_0/\varepsilon = 0.05$ if $a = r_W$ in the interaction potential (6). Thus, from different standpoints, we obtain that the interaction of an excess electron with environment is relatively weak at the atomic densities where the electron mobility has the maximum and the diffusion cross section of the electron on each core is also relatively small.

As follows from the above analysis, the gas model can be valid for the mobility of an excess electron in condensed inert gases in some range of atomic densities. This means that in the case where we compose the potential energy surface for an individual electron inside a condensed inert gas in the form of wells and hills, the amplitude of the electron scattering on an individual well or hill is less than the distance between the nearest neighboring atoms. We can also use another criterion of the gas model validity, the condition that the electron mean free path in a condensed inert gas is large compared to the distance between neighboring

atoms. This allows us to use the gas model for electron scattering, according to which an electron is scattered independently on neighboring nonuniformities of the potential energy surface. This leads to the classical theory of electron kinetics in gases in an external electric field in this case of an excess electron in condensed inert gases. This theory was elaborated for kinetics of electrons in semiconductors and gases [44–50]. It is represented in contemporary books [41, 51, 52], and we use this theory below for excitation of atoms in condensed inert gases.

Although the criterion of weakness of the interaction of an excess electron in condensed inert gases at high electron mobilities is fulfilled as well as the criterion of the gas approach for propagation of an excess electron, the character of electron motion is more complex in reality. Indeed, due to the exchange interaction of an excess electron with atomic electrons, an excess electron cannot penetrate the atoms. Hence, if we consider electron scattering on atomic cores to be independent, the cross section of scattering on each core is of the order of the atomic radius squared, which significantly exceeds the values in Table 4 that follow from the mobility data. Therefore, a large mean free path for electrons inside liquid inert gases may be explained by collective effects in simultaneous electron scattering on several cores, and the above gas model has a qualitative character. Nevertheless, we use the above gas model for the electron scattering in liquid inert gases as a result of the interaction with independent scatterers because of its simplicity.

4. EXCITATIONS IN CONDENSED INERT GASES BY ELECTRONS DRIFTING IN AN EXTERNAL ELECTRIC FIELD

In analyzing the electron behavior in a gas of independent scatterers, we use the classical theory [44–50] of electron motion in gases under the action of an external electric field. The basis of this theory is a small change of the electron energy at a remarkable change of the electron momentum as a result of elastic electron–atom scattering because of a small ratio of the electron and atom masses. This allows us to expand the velocity distribution function of the electron $f(\mathbf{v})$ over spherical harmonics, and this distribution function has the form

$$f(\mathbf{v}) = f_0(v) + v_x f_1(v), \quad (9)$$

where v_x is the electron velocity component along the electric field, and $v f_1(v) \ll f_0(v)$ according to the basic concept. Although the antisymmetric part of the

distribution function $f_1(v)$ is small, it is of importance because the electric field acts on electrons through this component of the distribution function. The set of equations for the distribution function in the case of only the elastic electron–atom scattering and in neglecting inelastic processes has the form (see, e.g., [51])

$$a \frac{df_0}{dv} = -\nu v f_1, \quad \frac{a}{3v^2} \frac{d}{dv} (v^3 f_1) = I_{ea}(f_0) \quad (10)$$

in the stationary case, where $a = eE/m_e$, E is the electric field strength, $\nu = Nv\sigma(v)$ is the rate of electron collisions with atoms, and $I_{ea}(f)$ is the electron–atom collision integral. This implies a general expression (2) for the electron mobility, where the average is taken over the spherical component f_0 of the distribution function.

We consider the simplest case where $\sigma(v) \sim 1/v$ and the rate ν is independent of v . We then obtain the expressions

$$f_0(\varepsilon) \sim \exp\left(-\frac{\varepsilon}{T_e}\right), \quad w = \frac{a}{\nu} = \frac{eE}{m_e \nu}, \quad (11)$$

$$T_e = T + \frac{M a^2}{3\nu^2},$$

where ε is the electron energy (which is to be used along with the electron velocity) and T is the gas temperature. We note that we ignore collisions between electrons, and the parameter T_e does not correspond to the definition of the electron temperature, but coincides with it in the expression for distribution function (11). The drift velocity is proportional to the electric field strength, and this dependence relates to liquid xenon as long as inelastic collisions are weak [53]. Hence, this simple dependence $\nu(v)$ describes the electron behavior in liquid xenon. On the contrary, the electron behavior in gaseous xenon is more complex because of a nonmonotonic velocity dependence for the electron–atom cross section due to the Ramsauer effect. Such a dependence leads to the maximum of the electron mobility as a function of the electric field strength [7], which also follows from detailed calculations [54] for gaseous xenon. Below, we use the simplest dependence $\sigma(v) \sim 1/v$ for the analysis of electron kinetics in liquid xenon.

Including excitation of atoms by electron impact into consideration and assuming that above the excitation threshold $\Delta\varepsilon$, the electron loses the energy by atom excitation, we obtain that the distribution function is zero at the excitation threshold $f_0(\Delta\varepsilon) = 0$. This gives the energy distribution function $f_0(\varepsilon)$ of an excess electron [55] in the form

$$f_0(\varepsilon) = \begin{cases} C [\varphi_0(\varepsilon) - \varphi_0(\Delta\varepsilon)] & \varepsilon \leq \Delta\varepsilon, \\ 0, & \varepsilon \geq \Delta\varepsilon, \end{cases} \quad (12)$$

where C is the normalization constant and $\varphi_0(\varepsilon)$ is given by formula (11),

$$\varphi_0(\varepsilon) = \exp\left(-\frac{\varepsilon}{T_e}\right). \quad (13)$$

In the regime under consideration, the drift velocity is proportional to the electric field strength E even at high fields, and the parameter $T_e \sim E^2$ at high fields, while the average electron energy is restricted by the value $(3/7)\Delta\varepsilon$ in the limit of high electric fields. In this regime, electrons acquire energy from the external field and spend it in elastic collisions with atoms. When an electron reaches the excitation energy $\Delta\varepsilon$, a forming excited atom emits a photon. The electron energy becomes zero after atom excitation, and the process of the increase of the electron energy repeats. Therefore, the rate of atom excitation is determined by the flux in the energy space, and on the basis of the indicated energy balance, we have the rate of atom excitation given by [16]

$$\frac{dN_*}{dt} = \frac{4}{\sqrt{\pi}} \left(\frac{\Delta\varepsilon}{T_e}\right)^{3/2} N_e \frac{m_e}{M} \nu \exp\left(-\frac{\Delta\varepsilon}{T_e}\right), \quad (14)$$

$$T \ll T_e \ll \Delta\varepsilon,$$

where N_* is the number density of excited atoms, N_e is the number density of excess electrons, and $\Delta\varepsilon$ is the atom excitation energy.

We now find the portion γ of the power acquired by the electrons from the external electric field and spent to atom excitation. We assume that the power acquired from the field is transformed below the excitation threshold mostly into the atom thermal energy as a result of elastic collisions between electrons and atoms, and this power per one electron is eEw , where w is the electron drift velocity. From formula (14), we then have

$$\gamma = \frac{\Delta\varepsilon \frac{dN_*}{dt}}{eEwN_e} = \frac{4}{3\sqrt{\pi}} \left(\frac{\Delta\varepsilon}{T_e}\right)^{3/2} \exp\left(-\frac{\Delta\varepsilon}{T_e}\right), \quad (15)$$

$$T \ll T_e \ll \Delta\varepsilon,$$

where

$$T_e = \frac{Ma^2}{3\nu^2} = \frac{Mw^2}{3}$$

is the effective electron temperature. Figure 2 gives the dependence of the efficiency of atom excitation γ on the electron energy $\bar{\varepsilon} = 3T_e/2$ under these conditions [16]. Formally, this expression has a maximum at $T_e = 2\Delta\varepsilon/5$, where $\xi = 0.61$, but because $\varepsilon \leq 3\Delta\varepsilon/7$, the above consideration is valid below this limit. It follows from (15) that the transformation efficiency γ is significant even at low values of $T_e/\Delta\varepsilon$.

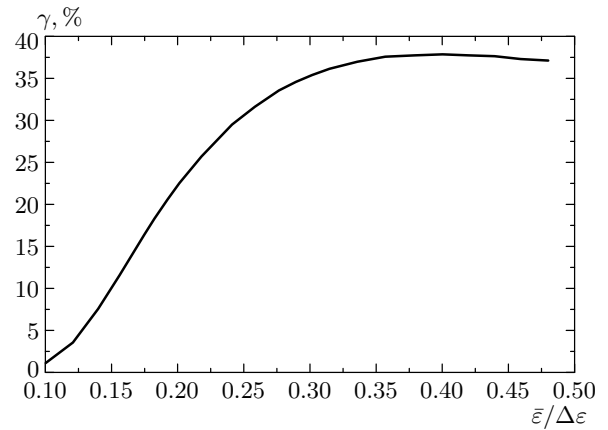


Fig. 2. The efficiency of excitation of atoms in an atomic system if the rate ν of the electron–atom elastic scattering is independent of the electron velocity v

In this consideration, we implicitly use the criterion

$$\nu_{ex} \gg \frac{m_e}{M} \nu,$$

where ν_{ex} is a typical excitation rate of atoms in collisions with a test electron. To obtain a more specific criterion, we analyze the other limiting case of slow atom excitation. The energy distribution function then has the form

$$f_0(\varepsilon) = C\varphi_0(\varepsilon)$$

and differs from that in formula (9) by the absence of decay of fast electrons in the excitation process. Correspondingly, the rate of the atom excitation is equal to [16, 41]

$$\frac{dN_*}{dt} = N_e N_a k_q \frac{g_*}{g_0} \exp\left(-\frac{\Delta\varepsilon}{T_e}\right), \quad (16)$$

where k_q is the rate constant of quenching resonantly excited atoms by a slow electron, and g_0 and g_* are the statistical weights of the ground and excited atomic states. We have used the principle of detailed balance between the excitation and inverse quenching processes [51, 56], which is convenient because the quenching rate constant is independent of the electron energy for a slow electron ($T_e \ll \Delta\varepsilon$). The values of the quenching rate constants for resonantly excited atoms of inert gases are given in Table 5. We there give the values of k_{el} for thermal collisions on the basis of the electron mobilities in gases according to the data in Table 1.

Comparing the excitation rates according to formulas (13) and (16), we find them to be simultaneously valid if the criterion

Table 5. Parameters of the lowest resonantly excited states of inert gas atoms [16, 56]

Atom (state)	$\Delta\varepsilon$, eV	J^* , eV	τ , ns	k_q , $10^{-9} \text{ cm}^3/\text{s}$	$1/k_q\tau$, 10^{16} cm^{-3}	k_{el} , $10^{-8} \text{ cm}^3/\text{s}$	$(m_e/M)k_{el}$, $10^{-14} \text{ cm}^3/\text{s}$
Ar ($1s_2$)	11.62	4.14	10	0.82	12	0.15	2.0
Ar ($1s_4$)	11.83	3.93	2	3.9	13		
Kr ($1s_2$)	10.03	3.97	3.5	3.9	7.3	2.8	18
Kr ($1s_4$)	10.64	3.36	3.2	3.5	8.9		
Xe ($1s_2$)	8.44	3.69	3.6	7.0	4.0	10	43
Xe ($1s_4$)	9.57	3.43	3.5	4.6	6.2		

$$k_q \gg \frac{m_e}{M} \left(\frac{\Delta\varepsilon}{T_e} \right)^{3/2} k_{el} \quad (17)$$

is satisfied, where the rate constant of the elastic electron–atom scattering is introduced as $k_{el} = \nu/N_a$. Using the gas model for elastic scattering of electrons on atoms, we take the quenching rate constants for electron–atom collisions and radiative times of excited atoms in a condensed inert gas to be close to those in a gas, whereas the rate constants for the elastic electron scattering are much less in condensed state. This means that criterion (17) is even more valid for condensed inert gases than for their gaseous phase. In addition, this leads to a high efficiency of transformation of the electric field energy into excitations in electronic excitation for condensed inert gases.

We note [57] that in spite of the simplicity of condensed inert gases as a system of bound atoms in the ground state (see Table 2), elementary excitations in this system — excitons — have a complex structure. One more peculiarity of excitons in condensed inert gases in comparison with excitations in a gaseous system is due to the interaction of an excited atom with the environment. In gases, excited atoms are formed as a result of the electron impact, and these excited atoms emit radiation. In condensed inert gases, an excited atom is transformed very fast into a diatomic excimer molecule and lives in such a form. Therefore, radiation of a condensed inert gas is characterized by a broad band for a quasimolecular exciton, and luminescence is shifted to the red side in comparison with the spectral line of atom emission, and one can expect the luminescence quantum yield to be close to unity.

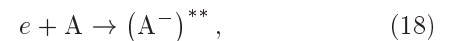
There are two types of quasimolecular excitons depending on the total spin of an excited electron and the core. Because the electron spin is zero for the ground state, the radiative time of an exciton with the total

spin one is much greater than the radiative time of an exciton with zero total spin [58]. This fact is taken into account in the analysis of exciton kinetics.

5. ROLE OF AUTODETACHING STATES IN GENERATION OF EXCITONS

Because of a weak electron–atom interaction in condensed inert gases for atomic densities of high electron mobility, an excess electron experiences a weak friction when it is drifting in an external electric field. Therefore, the efficiency is high for conversion of the electron energy obtained from the field into excitation of atoms. But this weak electron–matter interaction is the reason of a heightened role of autodetaching states in formation of excitons. We consider this problem in what follows.

Excitation and decay of autodetaching states in the course of motion of an excess electron in condensed inert gases proceeds according to the scheme



where A is the inert gas atom. The parameters of autodetaching states $(A^-)^{**}$ of inert gas negative ions are analogous to those of $H^-(2s^2)$ [59], where the autodetaching state is placed about 0.4 eV lower than the atom excitation energy, and the lifetime of these autodetaching states is approximately 10^{-14} – 10^{-13} s. Because a typical time of the radiative decay of an ionic state through the emission of a UV photon is about 10^{-9} – 10^{-8} s, its probability to occur during the decay of an autodetaching state is small. But this process can be repeated, and the process of photon emission through channel (18) may be remarkable. If channel (18) is realized, the spectrum of radiation is charac-

terized by longer wavelengths than that from A^* but shorter than from A_2^* [22].

Electron capture in an autodetaching state leads to an additional decrease of the electron distribution function, and the capture cross section σ_{res} is given by the Breight–Wigner formula [42]

$$\sigma_{res} = \frac{\pi\hbar^2}{2m_e\varepsilon} \frac{\Gamma^2}{(\varepsilon - \varepsilon_{res})^2 + \Gamma^2/4}, \quad (19)$$

where Γ is the width of the autodetaching level and ε_{res} is the electron energy for this resonance. We first determine a decrease of the energy distribution function of electrons formally, considering electron capture on the autodetaching level as the elastic electron scattering. We can then represent the cross section of the electron–atom elastic scattering as the sum of two parts,

$$\sigma = \sigma_0 + \sigma_{res}, \quad (20)$$

where σ_0 smoothly depends on the electron energy and σ_{res} is the resonant part of the elastic cross section. Restricting to the Druyvesteyn case of the electron distribution function [44], where a typical electron energy significantly exceeds the thermal energy of atoms, we obtain that instead of formula (12), the distribution function is given by

$$\varphi_0(\varepsilon) = \exp\left(-\int^\varepsilon d\varepsilon \left(\frac{Ma^2}{3\nu^2}\right)^{-1}\right). \quad (21)$$

If we assume the rate of elastic electron–atom scattering ν to be independent of the electron energy, formula (19) is transformed in formula (12) in neglecting the resonant part of electron scattering.

The character of the electron interaction with an autodetaching state consists in the electron capture on this level and in the subsequent decay of the resonance level, which can lead to a change of the direction of the electron velocity. Thus, the capture of an electron on the resonance level is similar to elastic scattering of the electron with a change of the direction of its motion. Assuming that $\sigma_{res} \gg \sigma_0$ at the resonance, we find that formation of the autodetaching state under the above consideration leads to a jump in the exponent (19), and this jump is equal to

$$\xi = \int^\varepsilon d\varepsilon \left(\frac{Ma^2}{3\nu_{res}^2}\right)^{-1}, \quad (22)$$

where $\nu_{res} = Nv\sigma_{res}$, which implies that above the resonance, the distribution function acquires the factor $\exp(-\xi)$. This means that distribution function (13) is transformed to the form

$$\varphi_0(\varepsilon) = \exp\left(-\frac{\varepsilon}{T_e}\right), \quad \varepsilon < \varepsilon_{res},$$

$$\varphi_0(\varepsilon) = \exp\left(-\frac{\varepsilon}{T_e} - \xi\right), \quad \varepsilon > \varepsilon_{res}.$$

Under the assumption that the rate ν of the electron–atom scattering is independent of ε , the exponent is given by

$$\xi = \int \frac{3d\varepsilon}{Ma^2} (Nv\sigma_{res})^2 = \frac{3\pi\Gamma}{4Ma^2} (Nk_{res})^2, \quad (23)$$

where

$$k_{res} = \frac{4\pi\hbar^2}{v_{res}}, \quad v_{res} = \sqrt{\frac{2\varepsilon_{res}}{m_e}}. \quad (24)$$

In particular, for $\varepsilon_{res} = 8$ eV (xenon), we obtain $k_{res} = 1.4 \cdot 10^{-7}$ cm³/s and this estimate is valid for both gaseous and condensed states when the gas model is applicable.

Thus, the role of the autodetaching level in electron kinetics is governed by exponent (23). Taking $k_{el} = \nu/N_a$, where k_{el} is the rate constant of the elastic electron–atom scattering aside the resonance, we obtain

$$\xi = \frac{\pi\Gamma}{4T_e} \left(\frac{k_{res}}{k_{el}}\right)^2. \quad (25)$$

Using formula (25) for estimate in gaseous and condensed xenon, we take $\Gamma \approx 0.01$ eV, $T_e \sim 3$ eV, $\varepsilon_{res} \approx 8$ eV, and the value of k_{el} from Table 5. This gives $\xi \approx 0.005$ for gaseous xenon, i.e., autodetaching states do not affect the electron distribution function there. Applying the gas model to condensed xenon, we can evaluate the rate constant of the electron–atom scattering from the known zero-field mobility of electrons as $k_{el} = 2.4 \cdot 10^{-11}$ cm³/s at the number density corresponding to the mobility maximum. Substituting this small rate constant in (25), we obtain $\xi \sim 10^5$. Thus, as supposed in [22], formation of autodetaching states is not essential for excitation of atoms in gases even at high atomic densities. But it may be important in condensed inert gases at densities where the electron mobility is high.

The autodetaching states are of importance in electron kinetics and atom excitation if $\xi \gg 1$, and we determine this limit below. The probability $dw(\varepsilon)$ of the electron energy to be in a range from ε to $\varepsilon + d\varepsilon$ after the decay of an autodetaching state according to formula (19) is given by

$$dw = \frac{ds}{\pi(1+s^2)}, \quad s = \frac{2(\varepsilon - \varepsilon_{res})}{\Gamma}. \quad (26)$$

We suppose that autodetaching is not essential if $\sigma_{res} \leq \sigma_0$, i.e., if

$$s^2 \geq s_0^2 = \frac{2\pi\hbar^2}{m_e\varepsilon_{res}\sigma_0}, \quad (27)$$

and the probability w that $s \geq s_0$, when the autode-taching state can be ignored, is equal to

$$w = \int_{s_0}^{\infty} dw = \frac{1}{\pi s_0}. \quad (28)$$

In particular, for xenon at the atomic number density of the maximum electron mobility, we have $s_0 \approx 14$. The presence of an autode-taching state therefore acts as a barrier in kinetics of electrons in the space of electron energy. In the case of xenon, the probability to pass through this barrier is approximately 0.02. Of course, this decreases the efficiency of transformation of the energy of the external electric field into the energy of emitting photons through electrons that excite atoms in condensed inert gases.

This effect decreases the efficiency γ of transformation of the electric field energy into the energy of VUV photons because it leads to a drop of the distribution function. But in the limit

$$T_e \gg \Delta\varepsilon - \varepsilon_{res}, \quad (29)$$

this influence on the efficiency coefficient γ is small if the criterion

$$wk_q \gg \frac{m_e}{M} \left(\frac{\Delta\varepsilon}{T_e} \right)^{3/2} k_{el} \quad (30)$$

is satisfied instead of criterion (17). Indeed, because $\Delta\varepsilon - \varepsilon_{res} \approx 0.4$ eV, criterion (29) is valid if the efficiency γ is not small. Next, both the influence of electron capture in the autode-taching state and the atom excitation lead to a decrease of the distribution function, but because these effects are not separated, all the fast electrons spend their energy to the excitation of atoms due to criterion (30). Thus, although autode-taching states affect the efficiency of exciton production by drifting the excess electrons in condensed inert gases, this is evidently not essential at optimal atomic densities. An indirect confirmation of this is the efficiency of 18% for conversion of the electric energy into VUV radiation that is observed in solid xenon [26, 27]. Formula (15) gives this value at $T_e = 2.5$ eV ($\Delta\varepsilon/T_e = 3.2$).

Because of high efficiency, it is profitable to create a self-maintaining electric discharge in condensed inert gases for generation of VUV photons, as suggested in [23, 24]. Such an emission was observed in liquid xenon [25] in the form of a broad line near the central wavelength of 175 nm when electrons were drifted from a cold field-emission cathode at moderate electric field strengths. Generation of VUV photons in solid xenon was achieved in experiments [26, 27]. As follows from the above analysis, the energy distribution

function of the excess electrons is zero at electron energies above the excitation threshold, and hence the direct ionization of atoms by electron impact is impossible in condensed inert gases. In addition, the number density of the excess electrons is relatively small, and stepwise ionization does not proceed in condensed inert gases. Therefore, to support a discharge, ionization processes are required outside a condensed inert gas. In particular, within the framework of the experimental scheme in [26, 27], a photocathode is placed near solid xenon, and secondary electrons are formed as a result of absorption of VUV photons by the photocathode. A gap filled with a gaseous xenon allows one to avoid the self-diffusion effect that decreases the probability of the electron entering a media in the case of a direct contact of the photocathode with condensed matter by several orders of magnitude [60]. In solid xenon of 1 mm thickness at the electric tension of 1 kV, approximately 20 photons may be formed per one electron. As a result, a self-maintaining discharge is created in this scheme.

We now make some evaluations for this scheme with a layer of condensed xenon and a layer of gaseous xenon that are governed separately because of using a grid. For definiteness, we take xenon at the triple point, such that the temperature is equal to 163 K and the pressure of gaseous xenon is 0.8 atm, which corresponds to the number density of xenon atoms approximately $4 \cdot 10^{19}$ cm⁻³. Taking the characteristic energy in liquid xenon about 3 eV, which provides the efficiency of conversion of the electric energy into VUV radiation about 20%, we obtain the electric field strength for liquid xenon approximately 100 V/cm. After passing the liquid layer, each electron creates 5 VUV photons per 1 cm of its way. The drift velocity of electrons in liquid xenon is $2 \cdot 10^5$ cm/s under these conditions. In the gaseous layer, the average energy 2 eV is attained at the reduced electric field strength $E/N \approx 1$ Td [54], which corresponds to 400 V/cm. We note that the number k of forming electrons per electron in a condensed inert gas is equal to

$$k = \frac{\gamma El}{\Delta\varepsilon}, \quad (31)$$

where l is the layer thickness. Therefore, it is profitable to increase the electric field strength in a layer of a condensed inert gas. This is not valid for a gaseous layer, because along with excitation processes, direct ionization of atoms by electron impact proceeds, which restricts both the layer thickness and the electric field strength. The total electric current density is limited by heat transport processes, and this value is measured in $\mu\text{A}/\text{cm}^2$.

On the basis of the experience of experimental

study [25–27] and from the above analysis, one can simplify the scheme of a self-maintaining electric discharge in a condensed inert gas and improve the discharge parameters if the electric discharge is a generator of VUV radiation. First, a CsI photocathode is useful for this goal, because its efficiency for the electron emission is almost 3 orders of magnitude higher at $\lambda = 172$ nm than that for a zinc photocathode [60] that was used in experiments [26, 27]. Second, it is convenient to apply an alternating voltage to a layer from condensed inert gases. In this manner, using a suitable frequency of the electric field ($f \approx 1$ MHz), one can increase the path that an electron passes in a layer. As a result, in a layer of a thickness of several mm, an electron passes the path of several meters. Next, because of the increase of the electron lifetime in a discharge, stepwise ionization processes may be important, increasing the electron number density. This allows improving the parameters of a self-maintaining electric discharge.

6. CONCLUSIONS

High electron mobility is observed in heavy condensed inert gases (Ar, Kr, Xe) in a narrow range of atomic densities. A widespread explanation of this effect [17–21] by the Ramsauer effect in the electron scattering on an individual atom is not correct because of a large distance of the electron–atom scattering in comparison with the distance between neighboring atoms at these atomic densities. We have shown that the nature of high electron mobility is connected with the transition from an attracting interaction potential to a repulsing one between an excess electron and the atom ensemble. High electron mobility is accompanied by weak electron interaction with atoms of a condensed inert gas, which allows us to use the gaseous model for electron scattering inside this system. In reality, electron scattering in condensed inert gases is not reduced to scattering on individual cores, i.e., collective effects are important in these processes. Therefore, a quantitative description is used in experimental results, and the parameters corresponding to the electron mobility maximum do not admit a similarity law for different inert gases. In addition, the analysis of electron kinetics in condensed inert gases in external fields shows that processes of formation of autodetaching states lead to a decrease of the electron energy distribution function with the increase of the electron energy. Nevertheless, formation of autodetaching states may be not essential for the transformation of the electric field energy into vacuum ultraviolet radiation if a condensed inert gas is transparent for the electron drift.

The results of this analysis can be used for creation

of a self-maintaining electric discharge in condensed inert gases as a generator of ultraviolet radiation. The basis of this is the existing versions of such a discharge [25–27] together with the above analysis of the nature of processes involving electrons. This allows us to make the next step to construct a new version of the self-maintaining electric discharge in condensed inert gases.

This work is supported in part by the Russian Foundation for Basic Research (grants № 04-03-32684 and LSS-1953.2003.2).

REFERENCES

1. H. Schnyders, S. A. Rice, and L. Meyer, *Phys. Rev.* **150**, 127 (1966).
2. B. Halpern et al., *Phys. Rev.* **156**, 351 (1967).
3. L. S. Mi, S. Howe, and W. Spear, *Phys. Rev.* **166**, 871 (1968).
4. J. A. Jahnke, L. Meyer, and S. A. Rice, *Phys. Rev. A* **3**, 734 (1971).
5. T. Kimura and G. R. Freeman, *Can. J. Phys.* **52**, 2220 (1974).
6. K. Yoshino, U. Sowada, and W. F. Schmidt, *Phys. Rev. A* **14**, 438 (1976).
7. S. S-S. Huang and G. R. Freeman, *J. Chem. Phys.* **68**, 1355 (1978).
8. S. S-S. Huang and G. R. Freeman, *Phys. Rev. A* **24**, 714 (1981).
9. R. Reiniger, U. Asaf, and I. T. Steinberg, *Chem. Phys. Lett.* **90**, 287 (1982).
10. E. M. Gushchin, A. A. Kruglov, and I. M. Obodovskii, *Zh. Eksp. Teor. Fiz.* **82**, 1114 (1982).
11. V. V. Dmitrienko, A. S. Romanuk, S. I. Suchkov, and Z. M. Uteshev, *Zh. Tekh. Fiz.* **53**, 2343 (1983).
12. R. Reiniger, U. Asaf, and I. T. Steinberg, *Zh. Tekh. Fiz.* **28**, 3193 (1983).
13. R. Reiniger et al., *Phys. Rev. B* **28**, 4426 (1983).
14. F. M. Jacobsen, N. Gee, and G. B. Freeman, *Phys. Rev. A* **34**, 2329 (1986).
15. A. K. Al-Omari, K. N. Altmann, and R. Reiniger, *J. Chem. Phys.* **105**, 1305 (1996).
16. B. M. Smirnov, *Uspekhi Fiz. Nauk* **172**, 1411 (2002).

17. J. Lekner, Phys. Rev. **158**, 130 (1967).
18. M. H. Cohen and J. Lekner, Phys. Rev. **158**, 305 (1967).
19. B. E. Springett, J. Jortner, and M. H. Cohen, J. Chem. Phys. **48**, 2720 (1968).
20. V. M. Atrazhev and I. T. Iakubov, J. Phys. C **14**, 5139 (1981).
21. V. M. Atrazhev and E. G. Dmitriev, J. Phys. C **18**, 1205 (1985).
22. E. B. Gordon and A. F. Shestakov, Low Temp. Phys. **27**, 883 (2001).
23. E. B. Gordon, O. S. Rzhetskii, and V. V. Khmelenko, Quant. Electr. **21**, 209 (1994).
24. E. B. Gordon, V. V. Khmelenko, and O. S. Rzhetskii, Chem. Phys. Lett. **217**, 605 (1994).
25. A. S. Schussler et al., Appl. Phys. Lett. **77**, 2786 (2000).
26. E. B. Gordon, G. Frossati, and A. Usenko, Zh. Eksp. Teor. Fiz. **123**, 846 (2003).
27. A. Usenko, G. Frossati, and E. B. Gordon, Phys. Rev. Lett. **90**, 153201 (2003).
28. B. M. Smirnov, Uspekhi Fiz. Nauk **171**, 1291 (2001).
29. R. A. Aziz and M. J. Slaman, Chem. Phys. **130**, 187 (1989).
30. A. K. Dham, A. R. Allnatt, W. J. Meath, and R. A. Aziz, Mol. Phys. **67**, 1291 (1989).
31. R. A. Aziz and M. J. Slaman, J. Chem. Phys. **92**, 1030 (1990).
32. A. K. Dham, W. J. Meath, A. R. Allnatt, R. A. Aziz, and M. J. Slaman, Chem. Phys. **142**, 173 (1990).
33. E. Clementi and C. Roetti, At. Data Nucl. Data Tabl. **14**, 177 (1974).
34. A. D. McLean and R. S. McLean, At. Data Nucl. Data Tabl. **26**, 197 (1981).
35. A. A. Radzig and B. M. Smirnov, *Reference Data for Atoms, Molecules, and Ions*, Springer, Berlin (1986).
36. E. Fermi, Nuovo Cim. **11**, 157 (1934).
37. R. S. Berry, in: *Theory of Atomic and Molecular Clusters*, ed. by J. Jellinek, Springer, Berlin (1999).
38. D. Wales, Adv. Chem. Phys. **115**, 1 (2000).
39. H. S. W. Massey, E. H. S. Burhop, and H. B. Gilbody, *Electronic and Ionic Impact Phenomena*, 2nd. ed., Clarendon Press, Oxford (1969).
40. L. G. H. Huxley and R. W. Crompton, *The Diffusion and Drift of Electrons in Gases*, John Wiley, New York (1974).
41. B. M. Smirnov, *Physics of Ionized Gases*, John Wiley, New York (2001).
42. L. D. Landau and E. M. Lifshitz, *Quantum Mechanics*, Nauka, Moscow (1976) (in Russian) [Oxford Univ. Press, Oxford (1980)].
43. A. J. Dahm, in *Progress in Low Temp. Phys.*, ed. by D. W. Brewer, North-Holland, Amsterdam (1985), vol. 9.
44. M. J. Druyvesteyn, Physica **10**, 61 (1930).
45. B. I. Davydov, Phys. Zs. Sowjetunion **8**, 59 (1935).
46. P. M. Morse, W. P. Allis, and E. P. Lamar, Phys. Rev. **48**, 412 (1935).
47. B. I. Davydov, Phys. Zs. Sowjetunion **12**, 269 (1937).
48. W. P. Allis and J. Allen, Phys. Rev. **52**, 703 (1937).
49. L. Ye. Gurevich, *Grounds of Physical Kinetics*, GITTL, Leningrad (1940) (in Russian).
50. W. P. Allis, Annal. der Phys. **21**, 383 (1956).
51. B. M. Smirnov, *Physics of Weakly Ionized Gas*, Nauka, Moscow (1972; 1978) (in Russian).
52. E. M. Lifshitz and L. P. Pitaevskii, *Physical Kinetics*, Nauka, Moscow (1979) (in Russian) [Pergamon Press, Oxford (1981)].
53. L. V. Lukin, Chem. Phys. **291**, 261 (2003).
54. V. M. Atrazhev, I. V. Chernysheva, and T. D. Doke, Jpn. J. Appl. Phys. **41**, 1572 (2002).
55. A. V. Eletskii and V. D. Kulagin, Fizika Plasmy **5**, 98 (1979).
56. B. M. Smirnov, *Physics of Atoms and Ions*, Springer, New York (2003).
57. I. Ya. Fugol, Adv. Phys. **27**, 1 (1978).
58. E. Morikawa et al., J. Chem. Phys. **91**, 469 (1989).
59. H. S. W. Massey, *Negative Ions*, Cambr. Univ. Press, Cambridge (1976).
60. E. Aprile et al., Nucl. Instr. and Meth. A **338**, 328 (1994).